ELSEVIER

Journal of Photochemistry and Photobiology A: Chemistry 145 (2001) 71–77

Journal of Photochemistry and Photobiology A:Chemistry

www.elsevier.com/locate/jphotochem

Vibronic couplings and radiationless transitions between the lowest 1Bu and the first excited 2Ag state of linear polyenes

P.O.J. Scherer, Sighart F. Fischer*

Technische Universität München, Theoretische Physik T38, Phsik I, Room 2077, 85748 Garching, Germany

Received 14 March 2001; received in revised form 1 June 2001; accepted 4 July 2001

Abstract

Transoctatetraene is studied as a model compound by means of ab initio (GAMESS) calculations to study the vibronic coupling between the lowest excited Ag state and the dipolar allowed second excited Bu state. It is found that the evaluated couplings to totally symmetric modes in combination to those of Bu-symmetry can describe the high resolution absorption excitation and emission spectra in more detail. The strong vibronic couplings can further explain the fast internal conversion between the 1Bu and the 2Ag state. It is argued that they can also induce a resonance energy transfer which can compete with a quadrupolar coupling at room temperature. The vibronic transfer mechanism is also discussed for photosynthetic systems including the transfer from carotenoids to bacteriochlorophylls. © 2001 Published by Elsevier Science B.V.

Keywords: Vibronic coupling; Transoctatetraene; Radiationless transitions

1. Introduction

Longer polyenes such as transoctatetraene have their lowest excited state as an optically forbidden state, which can be characterized as a double excited state. In the well-studied case of transoctatetraene [1] this is the 2Ag state. The lowest optically allowed state is 1Bu. It can be well characterized as a single excitation between the HOMO and the LUMO of the Hartree–Fock basis functions. Interestingly, the transition from the 1Bu state to the 2Ag state is very fast (200 fs) [2]. This is particularly important to understand the function of related molecules after excitation in biological systems such as carotenoids [3]. The 2Ag state is also involved in the fast isomerization of the retinal molecule of bacteriorhodopsin, even though here the external charge distribution plays a specific role [4,5].

Our calculations are based on the GAMESS program package [6]. We find one particular strongly coupling mode of Bu-symmetry which has a frequency of only 100 cm^{-1}. In combination with higher frequency totally symmetric modes it forms the most dominant progressions and can explain the rapid decay in the sub-picosecond regime. Moreover, we predict a temperature dependence of the rate which is mostly due to the thermal population of this mode.

The very strong vibronic coupling makes also resonance transfer between molecules conceivable, if the thermal population of such modes is considered. We find that this mechanism can compete with quadrupolar coupling mechanisms which have been analyzed for carotenoids to large extent [7,8].

2. Vibronic coupling parameters

The quantum calculations were done with the GAMESS program package [6] using a triple zeta basis set. First the ground state geometry was optimized on the Hartree–Fock SCF-level and normal modes were calculated. Then the geometry was deformed according to a zero point elongation Q_j^0 of the *j*th normal mode ω_j and the energies and transition dipoles of the two lowest singlet excitations $S_{1,2}$ were calculated using the GUGA CI routines with 10 active orbitals and up to triple excited configurations. Such calculations were performed for all of the normal modes. From these results, the vibronic coupling parameters were calculated as follows.

The linear coupling $\lambda_j\hbar\omega_j$ of the *j*th mode to the optical transition $S_0 \rightarrow S_{1,2}$ was calculated from the contribution of this mode to the reorganization energy

$$\lambda_{j1,2}^2\hbar\omega_j = \tfrac{1}{2}(E_{S_0\rightarrow S_{1,2}}(Q_j^0) - E_{S_0\rightarrow S_{1,2}}(-Q_j^0))$$

We found only very small asymmetries of the transition energies with respect to the sign of the normal mode elongation.

---

* Corresponding author. Tel.: +49-89-289-12373;
fax: +49-89-289-12444.
E-mail address: fisher@jupiter.t30.physik.tu-muenchen.de (S.F. Fischer).

1010-6030/01/$ – see front matter © 2001 Published by Elsevier Science B.V.
PII: S1010-6030(01)00571-8

Essentially, there is some indication for small frequency changes in the excited states for most of the modes which will be neglected in our analysis.

To calculate the vibronically induced coupling between S_1 and S_2 we used a simple model of two crossing adiabatic states of different symmetry (Ag and Bu) and neglected the coupling to higher excitations which will not change so significantly in the vicinity of the S_1–S_2 crossing.

As a function of the elongation of an asymmetric normal mode the adiabatic states are the eigenvectors of the interaction matrix

$$H=\begin{bmatrix} E_{2\mathrm{Ag}} & V(\{Q_j\}) \\ V(\{Q_j\}) & E_{1\mathrm{Bu}} \end{bmatrix}$$

At the ground state geometry, the two states are uncoupled, i.e. $V(0)=0$. Then in first order, we make use of a linear approximation

$$H=\begin{bmatrix} E_{2\mathrm{Ag}} & \sum_j \eta_j \dfrac{Q_j}{Q_j^0} \\ \sum_j \eta_j \dfrac{Q_j}{Q_j^0} & E_{1\mathrm{Bu}} \end{bmatrix}$$

At a geometry where the jth asymmetric mode is elongated with a zero point amplitude the transition to the Ag state borrows some intensity from the allowed transition to the Bu state. From this, we deduce the eigenvectors of the two adiabatic states

$$\begin{pmatrix} c \\ s \end{pmatrix} \quad \text{and} \quad \begin{pmatrix} -s \\ c \end{pmatrix} \quad \text{with}\, c=\frac{\sqrt{I_2}}{\sqrt{I_1+I_2}},$$

$$s=\pm\frac{\sqrt{I_1}}{\sqrt{I_1+I_2}}$$

After a simple orthogonal transformation with the help of these eigenvectors the coupling η_j is given by

$$\eta_j=cs(E_1(Q_j^0)-E_2(Q_j^0))=\frac{\sqrt{I_1 I_2}}{I_1+I_2}(E_1(Q_j^0)-E_2(Q_j^0))$$

3. Vibronically induced transitions

Since the calculation of excited state normal modes consumes too much computing power, we use a simplified approach [9,10] which neglects frequency changes and normal mode mixing in the excited states and starts from the harmonic approximation of the ground state modes

$$h_{\mathrm{S}_0}=\sum \hbar\omega_j\left(b_j^+ b_j+\frac{1}{2}\right)$$

The excited state vibrations are approximated in first order by shifted harmonic oscillators

$$h_{\mathrm{S}_n}=\sum \hbar\omega_j\left((b_j^+ +\lambda_{jn})(b_j+\lambda_{jn})+\frac{1}{2}\right)$$

where for antisymmetric modes $\lambda_{jn}=0$ and for the symmetric modes λ_{jn}^2 is given in Table 1.

Table 1

Calculated frequencies and coupling parameters $\lambda_{j1,2}^2$ of the symmetric modes. Several only weakly coupling modes in the 3000 cm^{-1} region are omitted. Couplings below 0.01 are not shown

Mode	Frequency (cm^{-1})	λ_{j1}^2	λ_{j2}^2	$(\lambda_{j1}-\lambda_{j2})^2$
1a	64	0.033	0.16	0.046
2a	179			
3a	241			
4a	246	0.108	0.36	0.074
5a	366			
6a	597	0.035	0.36	0.171
7a	1053	0.043	0.27	0.097
8a	1207	0.051	0.19	0.043
9a	1308	0.493	1.83	0.421
10a	1437	0.079	0.33	0.086
11a	1455	0.020	0.10	0.030
12a	1462	0.002	0.04	0.025
13a	1598	0.011	0.12	0.057
14a	1795	0.004	0.19	0.137
15a	1845	1.12	4.11	0.938

3.1. *Absorption of the allowed* 1Ag → 1Bu *transition*

Using the Franck–Condon approximation, the absorption intensity of the 1Ag → 1Bu transition at photon energy E is given by a thermal average of the ground state vibrations and a summation over the excited state vibrations as

$$I_{1\mathrm{Ag}\to 1\mathrm{Bu}}(E) = \frac{M^2}{Z}\sum \exp\left\{-\frac{1}{kT}\sum n_{j\mathrm{S}_0}\hbar\omega_j\right\}\left|\prod\langle n_{j\mathrm{S}_0}|n_{j\mathrm{Bu}}\rangle\right|^2 \times\delta\left(E-E_{1\mathrm{Bu}}^0+E_{1\mathrm{Ag}}^0-\sum(n_{j\mathrm{Bu}}-n_{j\mathrm{S}_0})\hbar\omega_j\right)$$

with the partition function $Z=\sum\exp\{-(1/kT)\sum n_{j\mathrm{S}_0}\hbar\omega_j\}$.

At low temperatures the contribution of hot bands can be neglected and the spectrum simplifies to

$$I_{1\mathrm{Ag}\to 1\mathrm{Bu}}(E)\approx M^2\sum\left|\prod\langle 0_{j\mathrm{S}_0}|n_{j\mathrm{Bu}}\rangle\right|^2 \times\delta\left(E-E_{1\mathrm{Bu}}^0+E_{1\mathrm{Ag}}^0-\sum n_{j\mathrm{Bu}}\hbar\omega_j\right)$$

where the Franck–Condon factors $\langle n_{j\mathrm{S}_0}|n_{j\mathrm{Bu}}\rangle$ can be evaluated easily for shifted harmonic oscillators. M is the electronic transition dipole moment of the 1Ag → 1Bu transition.

The upper part of Fig. 1 shows the resulting spectrum which is very similar to the experimental data from Hudson and Kohler which are shown in comparison with Fig. 2.

3.2. *Absorption of the forbidden* 1Ag → 2Ag *transition*

We treat the vibronic coupling of the antisymmetric modes in lowest order perturbation theory. A vibronic state in the 2Ag manifold has an admixture from the 1Bu manifold which induces a weak oscillator strength to the 1Ag → 2Ag

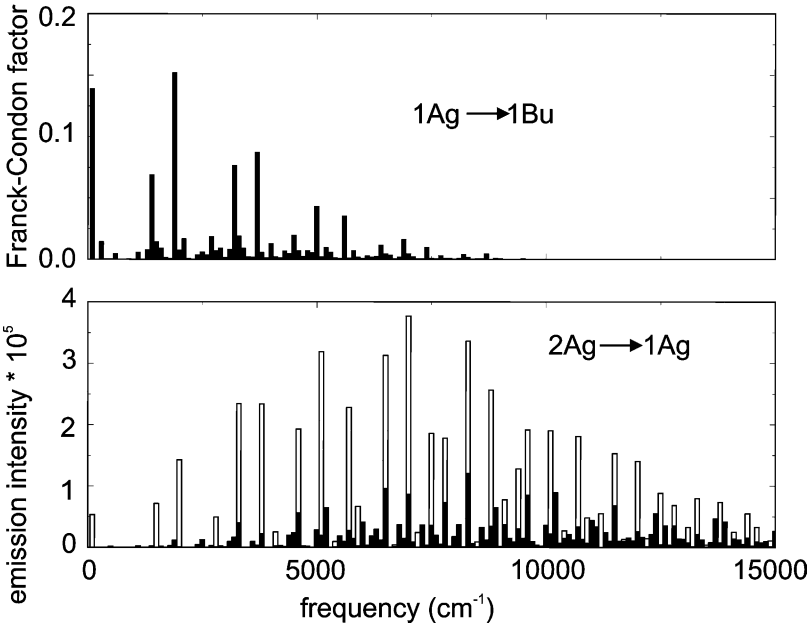

Fig. 1. Top: the bars show position and intensity (Franck–Condon factors) of the calculated absorption transitions; bottom: the bars show the position and intensity of the calculated emission spectrum. Hollow bars show the total intensities summed up within 100 cm^{-1}, whereas the full bars show the contribution of higher frequency promoting modes above 1b.

transitions. At low temperatures, intensity comes only from transitions with zero occupation of antisymmetric modes and is borrowed to transitions in the 2Ag manifold where exactly one antisymmetric quantum ω_p is excited:

$$\psi_{2\mathrm{Ag}} = |2\mathrm{Ag}, n_{j2\mathrm{Ag}} \cdots 1_p\rangle + \sum \frac{\eta_p}{\Delta - \hbar\omega_p + \sum(n_{j1\mathrm{Bu}} - n_{j2\mathrm{Ag}})\hbar\omega_j} \times \prod \langle n_{j1\mathrm{Bu}}|n_{j2\mathrm{Ag}}\rangle |1\mathrm{Bu}, n_{j\mathrm{Bu}} \cdots 0_p\rangle$$

$$I_{1\mathrm{Ag}\to 2\mathrm{Ag}}(E) = M^2 \sum \left(\frac{\eta_p}{\Delta - \hbar\omega_p + \sum(n_{j1\mathrm{Bu}} - n_{j2\mathrm{Ag}})\hbar\omega_j} \right)^2 \times \prod \langle n_{j1\mathrm{Bu}}|n_{j2\mathrm{Ag}}\rangle^2 \prod \langle 0_{j1\mathrm{Ag}}|n_{j1\mathrm{Bu}}\rangle^2 \times \delta\left(E - E^0_{2\mathrm{Ag}} + E^0_{1\mathrm{Ag}} - \hbar\omega_p - \sum(n_{j2\mathrm{Ag}} - n_{j1\mathrm{Ag}})\hbar\omega_j\right)$$

The intensity of the lowest transition at low temperatures which is the $0_{1\mathrm{b}} \to 1_{1\mathrm{b}}$ transition is a measure of the

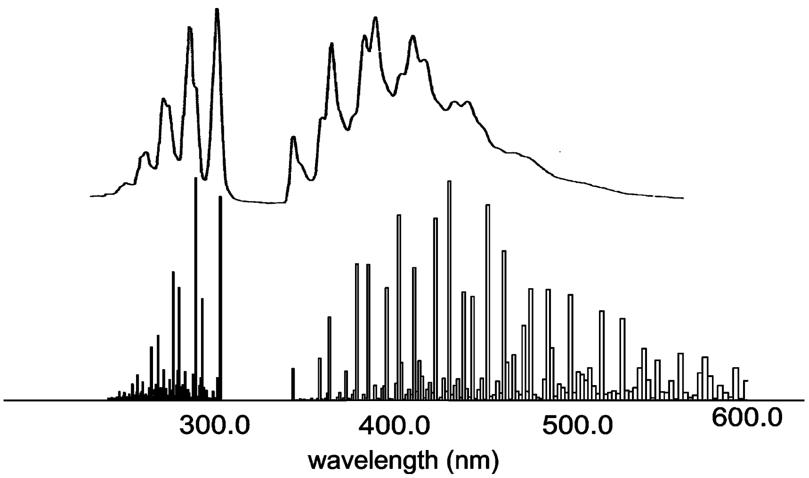

Fig. 2. The calculated vibronic profiles (bars) of the 1Ag → 1Bu absorption and the 2Ag → 1Ag emission are compared with experimental data of Hudson and Kohler (solid line). The calculated frequencies are scaled by a factor of 0.8 to account for the overestimation of the frequencies.

Table 2
Calculated frequencies and coupling parameters η_j of the antisymmetric modes

Mode	Frequency (cm^{-1})	η_j (cm^{-1})
1b	98	168
2b	153	0.3
3b	371	0.6
4b	433	36
5b	619	57
6b	704	2.3
7b	751	0.7
8b	988	1.9
9b	1020	49
10b	1056	1.4
11b	1065	1.0
12b	1083	0.5
13b	1100	0.3
14b	1119	3.3
15b	1146	0.3
17b	1157	2.0
18b	1251	53
19b	1385	47
20b	1442	119
21b	1468	29
22b	1577	1.8
23b	1749	65
24b	1837	123
25b	3247	18
26b	3252	59
27b	3283	49

vibronic coupling strength $\eta_{1\mathrm{b}}$ (Table 2)

$$I_{1\mathrm{Ag}\to 2\mathrm{Ag}}(\hbar\omega_{1\mathrm{b}}) \approx M^2 \frac{\eta_{1\mathrm{b}}^2}{\Delta^2} \prod \langle 0_{j1\mathrm{Ag}} | 0_{j2\mathrm{Ag}} \rangle^2$$

For an energy gap of 4000 cm^{-1}, a total Franck–Condon factor of 0.01 and a coupling of 150 cm^{-1} the resulting intensity of $\approx 1.5 \times 10^{-5}$ is quite comparable to the data of Hudson and Kohler. At higher energies the intensity increases rapidly due to the resonant denominator. The calculated spectrum is shown in Fig. 3.

3.3. *Emission of the forbidden* 2Ag → 1Ag *transition*

The reverse transition is treated in the same way as in Section 3.2. Neglecting thermal occupation of vibrations, we have

$$\psi_{2\mathrm{Ag}} = |2\mathrm{Ag}, 0_{j2\mathrm{Ag}} \cdots 1_k\rangle + \sum \frac{\eta_p}{\Delta - \hbar\omega_p + \sum n_{j1\mathrm{Bu}}\hbar\omega_j} \times \prod \langle 0_{j2\mathrm{Ag}} | n_{j1\mathrm{Bu}} \rangle |1\mathrm{Bu}, n_{j\mathrm{Bu}} \cdots 0_p\rangle$$

$$I_{2\mathrm{Ag}\to 1\mathrm{Ag}}(E) = M^2 \sum \left(\frac{\eta_p}{\Delta - \hbar\omega_p + \sum n_{j1\mathrm{Bu}}\hbar\omega_j} \right)^2 \times \prod \langle n_{j1\mathrm{Bu}} | 0_{j2\mathrm{Ag}} \rangle^2 \prod \langle n_{j1\mathrm{Ag}} | n_{j1\mathrm{Bu}} \rangle^2 \times \delta\left(E - \Delta - \hbar\omega_p - \sum n_{j1\mathrm{Ag}}\hbar\omega_j \right)$$

Thus the emission spectrum is the superposition of contributions from the antisymmetric promoting modes ω_p.

In a rough approximation for the limit of a large energy gap $\Delta = E^0_{1\mathrm{Bu}} - E^0_{2\mathrm{Ag}}$, we replace the denominator by an effective gap $\tilde{\Delta}$ and have

$$I_{2\mathrm{Ag}\to 1\mathrm{Ag}}(E) \approx M^2 \sum_p \left(\frac{\eta_p}{\tilde{\Delta}} \right)^2 \sum_{\{n_j\}} \prod \langle 0_{j2\mathrm{Ag}} | n_{j1\mathrm{Ag}} \rangle^2 \times \delta\left(E - \Delta - \hbar\omega_p - \sum n_{j1\mathrm{Ag}}\hbar\omega_j \right)$$

that is the total intensity is approximately $I_{2\mathrm{Ag}\to 1\mathrm{Ag}} \approx M^2(\sum \eta_k^2)/\tilde{\Delta}$ and the vibronic structure is essentially determined by the vibronic couplings λ_{j2}.

Two symmetric modes with calculated frequencies of 1308 and 1845 cm^{-1} show very large vibronic coupling to the electronic transitions. Interestingly, the coupling λ_{j2} to the transition 1Ag → 2Ag is approximately twice the coupling λ_{j1} to the transition 1Ag → 1Bu. Our results reveal that this is related to the fact that the state 2Ag contains large admixture of configurations with two excited

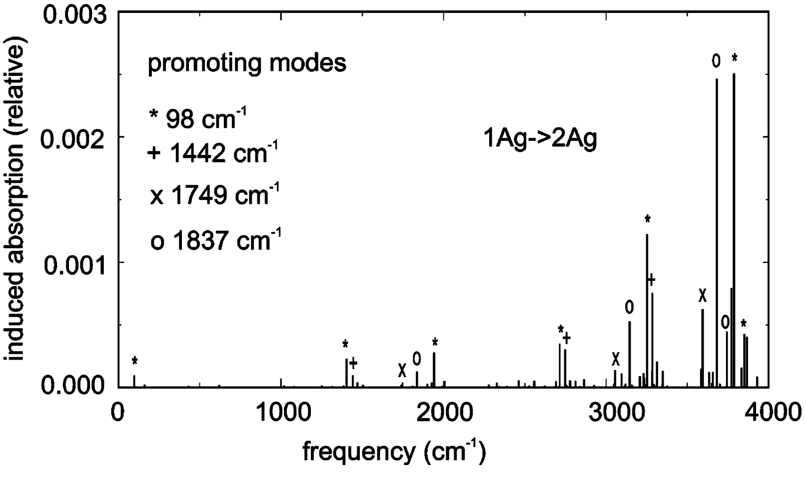

Fig. 3. The calculated transitions of the forbidden 1Ag → 2Ag absorption are shown as bars. Different symbols indicate the relevant promoting modes.

Table 3
Assignment of vibronic bands. Experimental data are extracted from [11] with an uncertainty of approximately ±50 cm^{-1}. Calculated intensities are relative to the 0–0 transition

Emission	Absorption	Calculated energy (cm^{-1})	Calculated absorption intensity	n_{9a}	n_{15a}
1150	1000	1308	0.49	1	0
1550	1550	1845	1.1	0	1
		2616	0.12	2	0
2700	2850	3153	0.55	1	1
3100	3150	3690	0.63	0	2
		3924	0.02	3	0
3950		4461	0.14	2	1
4300	4300	4998	0.31	1	2
4650	4600	5535	0.24	0	3
		5232	0.002	4	0
		5769	0.02	3	1
		6306	0.008	2	2
5500		6843	0.12	1	3
5900	5950	7380	0.07	0	4

electrons. The calculated vibronic structure is quite similar to the experimental absorption and emission spectra. The calculated frequencies are, however, too large by some 300 cm^{-1} which is quite common for ab initio calculations on the HF level. The calculated vibronic couplings also are somewhat too large. The calculated 0–1 transition of the 1845 cm^{-1} vibration has 10% more intensity than the 0–0 transition, whereas in the experimental absorption this ratio is approximately reversed (Table 3). For the 1308 cm^{-1} vibration the calculated intensity is 49% of the 0–0 transition which agrees quite well with the absorption spectrum where it appears as a shoulder of the second vibronic band at room temperatures.

For the emission spectrum, the situation is more complicated since several promoting modes contribute significantly. We found that the strongest contribution is from the lowest promoting mode 1b at 98 cm^{-1} (see lower part of Fig. 1). Transitions between electronic states of the same symmetry are only allowed if they are combined with excitation or de-excitation of an odd number of quanta of asymmetric modes. Therefore, the highest allowed transition in the emission spectrum is the $(n_{1b} = 0) \rightarrow (n_{1b} = 1)$ transition which is by $\hbar\omega_{1b}$ below the 0–0 transition. A similar argument applies for the vibronically induced absorption spectrum of the reverse transition 1Ag → 2Ag. Here, the lowest allowed transition creates one quantum of the 1b mode and is $\hbar\omega_{1b}$ above the 0–0 transition. This agrees quite well with the high resolution experiments [11] where the first bands of the 1Ag → 2Ag excitation spectrum and the 2Ag → 1Ag emission spectrum are separated by 210 cm^{-1} quite close to the calculated value of $2\hbar\omega_{1b} = 196\,\mathrm{cm}^{-1}$.

Since the 1b mode is the only coupling mode with $\hbar\omega < kT$ at room temperature we like to discuss some implications for the temperature dependence. With thermal occupation of the 1b mode two types of transitions are possible, namely excitation or de-excitation of a quantum $\hbar\omega_{1b}$. Since the induced coupling between the two electronically excited states increases with the amplitude of the vibration at higher temperatures also the fluorescence intensity is expected to increase.

Neglecting thermal occupation of other modes the temperature dependent emission spectrum is given by

$$\begin{aligned}
I_{2\mathrm{Ag}\to 1\mathrm{Ag}}(E, kT) &= \frac{1}{1-\exp(-\hbar\omega_{1b}/kT)} M^2 \\
&\quad\times \sum \left(\frac{\eta_{1b}}{\Delta - \hbar\omega_{1b} + \sum n_{j1\mathrm{Bu}}\hbar\omega_j} \right)^2 \\
&\quad\times \prod \langle n_{j1\mathrm{Bu}} | 0_{j2\mathrm{Ag}} \rangle^2 \prod \langle n_{j1\mathrm{Ag}} | n_{j1\mathrm{Bu}} \rangle^2 \\
&\quad\times \delta\left(E - \Delta - \hbar\omega_{1b} - \sum n_{j1\mathrm{Ag}}\hbar\omega_j \right) \\
&\quad+ \frac{\exp(-\hbar\omega_{1b}/kT)}{1-\exp(-\hbar\omega_{1b}/kT)} M^2 \\
&\quad\times \sum \left(\frac{\eta_{1b}}{\Delta + \hbar\omega_{1b} + \sum n_{j1\mathrm{Bu}}\hbar\omega_j} \right)^2 \\
&\quad\times \prod \langle n_{j1\mathrm{Bu}} | 0_{j2\mathrm{Ag}} \rangle^2 \prod \langle n_{j1\mathrm{Ag}} | n_{j1\mathrm{Bu}} \rangle^2 \\
&\quad\times \delta\left(E - \Delta + \hbar\omega_{1b} - \sum n_{j1\mathrm{Ag}}\hbar\omega_j \right) \\
&\quad+ M^2 \sum \left(\frac{\eta_p}{\Delta - \hbar\omega_p + \sum n_{j1\mathrm{Bu}}\hbar\omega_j} \right)^2 \\
&\quad\times \prod \langle n_{j1\mathrm{Bu}} | 0_{j2\mathrm{Ag}} \rangle^2 \prod \langle n_{j1\mathrm{Ag}} | n_{j1\mathrm{Bu}} \rangle^2 \\
&\quad\times \delta\left(E - \Delta - \hbar\omega_p - \sum n_{j1\mathrm{Ag}}\hbar\omega_j \right)
\end{aligned}$$

At room temperature, the first summand is enhanced by a factor of 2.7, whereas the prefactor of the second contribution is 1.7. The total emission intensity is approximately given by

$$\begin{aligned}
I_{2\mathrm{Ag}\to 1\mathrm{Ag}} &\approx M^2 \prod \langle n_{j1\mathrm{Ag}} | 0_{j2\mathrm{Ag}} \rangle^2 \\
&\quad\times \left(\coth\left(\frac{\hbar\omega_{1b}}{2kT} \right) \frac{\eta_{1b}^2}{\tilde{\Delta}^2} + \frac{\sum_{p\neq 1b} \eta_p^2}{\tilde{\Delta}^2} \right)
\end{aligned}$$

Using the same parameter values as above (Section 3.2), the estimated transition dipole is about 10^{-2} times that of the allowed 1Bu → 1Ag transition. Hence a Förster type transfer of excitation energy becomes conceivable where the intensity of the donor is vibronically induced by thermal population of low frequency modes. For carotenoids, this would become competitive to a quadrupole–dipole coupling mechanism at distances larger than about 10 Å as estimated from the calculated transition moments of Nagae et al. [7].

3.4. Radiationless transitions

There is an experimental evidence that after optical excitation of the 1Bu state radiationless transitions into the 2Ag state take place on the sub-picosecond time scale [2]. In the following, we want to calculate a simple rate expression based on the Golden Rule approximation and show that

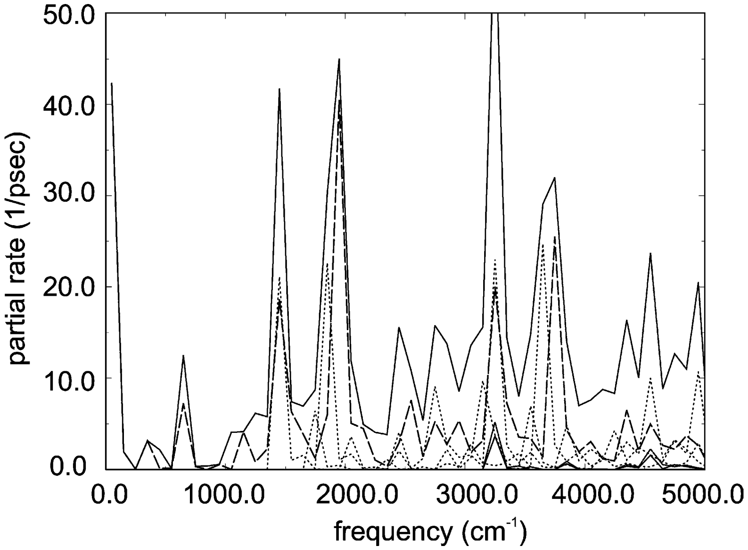

Fig. 4. The calculated rate of the radiationless transition 1Bu → 2Ag is shown as a function of the energy gap (solid line) together with its decomposition into contributions of different promoting modes (dotted lines). The dashed line shows the contribution of the lowest promoting mode 1b.

our calculated vibronic couplings are consistent with such ultra-fast processes. Starting from the rate expression

$$k = \frac{2\pi}{\hbar}\sum_{if}\frac{\exp(-E_i/kT)}{Z}V_{if}^2\delta(E_f - E_i)$$

again we first neglect thermal occupation of vibrations in the 1Bu state and apply the Franck–Condon approximation to have

$$k = \frac{2\pi}{\hbar}\sum \eta_p^2\langle 0_{j1\mathrm{Bu}}|n_{j2\mathrm{Ag}}\rangle^2 \times \delta\left(\Delta + \sum \hbar\omega_j(n_{j1\mathrm{Bu}} - n_{j2\mathrm{Ag}}) - \hbar\omega_p\right)$$

Considering thermal occupation of the 1b mode similar arguments as for the emission spectrum hold and give a thermal enhancement of the contributions from the 1b mode.

Fig. 4 shows the partial rates of the different promoting modes and their sum as a function of the energy gap. For values in the range of 3000–4000 cm^{-1} which are reasonable for octatetraene, the calculated rate falls easily into the sub-picosecond regime. At room temperature thermal occupation of the 1b mode enhances the rate by a factor of about 4 (see Fig. 5).

4. Summary

We have shown that the vibronic structure of transoctatetraene can be well explained on the basis of the vibronic

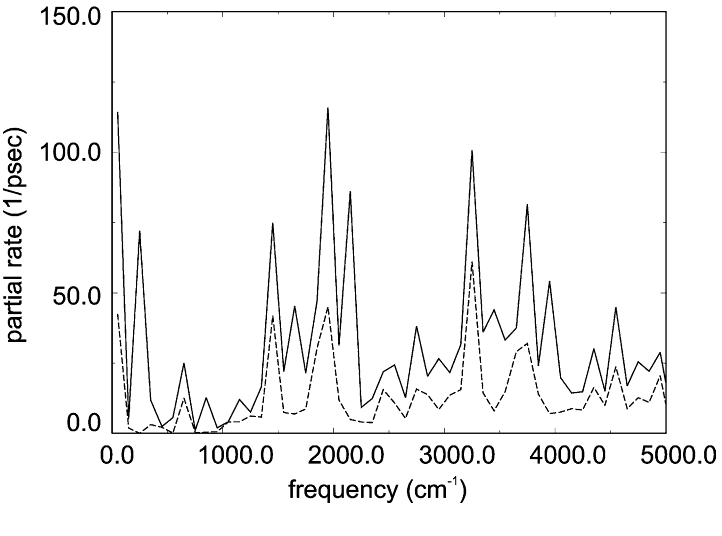

Fig. 5. The enhancement of the rate due to thermal population of the 1b mode at room temperature is shown (full line). The broken line shows the low temperature rate as in Fig. 4.

couplings between the two lowest excited states 1Bu and 2Ag. The modes of Bu-symmetry give rise to different series with progressions due to the couplings to the totally symmetric modes. Also, the radiationless transitions can be understood as a sum over different channels with the low frequency mode 1Bu being the most important. Similarly, strong vibronic coupling to an asymmetric low frequency mode has been discussed for diphenylhexatriene [12]. The fast transition is also due to the fact that the totally symmetric modes have a strong displacement of their equilibrium position in the 2Ag state with regard to the 1Bu state.

On the basis of these findings, we were able to identify a new efficient excitation transfer mechanism, which is of the Förster type and starts from vibronically excited promoting modes.

References

[1] B.F. Kohler, Chem. Rev. 93 (1993) 41–54.

[2] A.P. Shreve, J.K. Trautman, T.G. Owens, A.C. Albrecht, Chem. Phys. Lett. 178 (1991) 89.

[3] A. Domjanovic, T. Ritz, K. Schulten, Phys. Rev. E 9 (1999) 3293.

[4] M. Nonella, J. Phys. Chem. B 104 (2000) 11379–11388.

[5] F. Molner, M. Ben-Nun, T.J. Martinez, K. Schulten, J. Mol. Struct. (Theochem.) 506 (2000) 169–178.

[6] M.W. Schmidt, K.K. Baldridge, J.A. Boatz, S.T. Elbert, M.S. Gordon, J.J. Jensen, S. Koseki, N. Matsunaga, K.A. Nguyen, S. Su, T.L. Windus, M. Dupuis, J.A. Montgomery, J. Comput. Chem. 14 (1993) 1347–1363.

[7] H. Nagae, T. Kakitani, T. Katoh, M. Mimuro, J. Chem. Phys. 98 (1993) 8012.

[8] G.D. Scholes, R.D. Harcourt, G.R. Fleming, J. Phys. Chem. B 101 (1997) 7302–7312.

[9] P. Macak, Yi. Luo, H. Agren, Chem. Phys. Lett. 330 (2000) 447–456.

[10] P.O.J. Scherer, J. Phys. Chem. A 104 (2000) 6301–6307.

[11] B. Hudson, B. Kohler, Syn. Met. 9 (1984) 241–253.

[12] M. Pfeiffer, W. Werncke, S. Hogiu, A. Kummrow, A. Lau, Chem. Phys. Lett. 295 (1998) 56–62.